ARL-TR-8787 ● SEP 2019

DEVCOM ARMY RESEARCH LABORATORY

# Design and Implementation of a Terahertz (THz) Tomography System

by Geoffrey Xiao, Daniel Shreiber, and Carli Marsico

## NOTICES

### Disclaimers

The findings in this report are not to be construed as an official Department of the Army position unless so designated by other authorized documents.

Citation of manufacturer's or trade names does not constitute an official endorsement or approval of the use thereof.

Destroy this report when it is no longer needed. Do not return it to the originator.

ARL-TR-8787 ● SEP 2019


# Design and Implementation of a Terahertz (THz) Tomography System

**by Geoffrey Xiao and Carli Marsico**
***Drexel University, Philadelphia, PA***

**Daniel Shreiber**
***Weapons and Materials Research Directorate, CCDC Army Research Laboratory***

# REPORT DOCUMENTATION PAGE

*Form Approved*
*OMB No. 0704-0188*



| 1. REPORT DATE *(DD-MM-YYYY)* | 2. REPORT TYPE | 3. DATES COVERED (From - To) |
|---|---|---|
| September 2019 | Technical Report. | May–August 2018 |

**4. TITLE AND SUBTITLE**
Design and Implementation of a Terahertz (THz) Tomography System

**5a. CONTRACT NUMBER**

**5b. GRANT NUMBER**

**5c. PROGRAM ELEMENT NUMBER**

**6. AUTHOR(S)**
Geoffrey Xiao, Daniel Shreiber, and Carli Marsico

**5d. PROJECT NUMBER**

**5e. TASK NUMBER**

**5f. WORK UNIT NUMBER**

**7. PERFORMING ORGANIZATION NAME(S) AND ADDRESS(ES)**
CCDC Army Research Laboratory
ATTN: FCDD-RLW-ME
Aberdeen Proving Ground, MD 21005

**8. PERFORMING ORGANIZATION REPORT NUMBER**
ARL-TR-8787

**9. SPONSORING/MONITORING AGENCY NAME(S) AND ADDRESS(ES)**

**10. SPONSOR/MONITOR'S ACRONYM(S)**

**11. SPONSOR/MONITOR'S REPORT NUMBER(S)**

**12. DISTRIBUTION/AVAILABILITY STATEMENT**
Approved for public release; distribution is unlimited.

**13. SUPPLEMENTARY NOTES**

**14. ABSTRACT**

Tomography is an imaging technique that allows for the reconstruction of the internal structure of objects. Conventional magnetic resonance imaging (MRI) and X-ray computed tomography (CT) scans use tomography to create 3-D reconstructions of samples. Terahertz (THz) time domain spectroscopy (TDS), however, offers an alternative to MRI and CT due to its low-energy, non-ionizing radiation, and reasonable penetration lengths. This work presents an operational THz-TDS-based tomography setup, demonstrates its capabilities and explores some limitations. Theoretical background for the THz-TDS based tomography and possible explanations of the limitations are provided.

**15. SUBJECT TERMS**
THz-TDS, tomography, THz spectrum, nondestructive evaluation, X-ray microtomography

| 16. SECURITY CLASSIFICATION OF: | | | 17. LIMITATION OF ABSTRACT | 18. NUMBER OF PAGES | 19a. NAME OF RESPONSIBLE PERSON |
|---|---|---|---|---|---|
| a. REPORT | b. ABSTRACT | c. THIS PAGE | | | Daniel Shreiber |
| Unclassified | Unclassified | Unclassified | UU | 15 | 19b. TELEPHONE NUMBER (Include area code) (410) 306-4928 |

## Contents

## List of Figures

## 1. Introduction

Tomography is an imaging technique that allows for the reconstruction of the internal structure of objects. Conventional magnetic resonance imaging (MRI) and X-ray computed tomography (CT) scans use tomography to create 3-D reconstructions of samples.[1] Terahertz (THz) time domain spectroscopy (TDS), however, offers an alternative to MRI and CT due to its low-energy, non-ionizing radiation and reasonable penetration lengths.[2]

THz tomography systems have been used to analyze various materials and study 3-D shapes.[3–5] The field of tomography has also been well established in widely used techniques as MRI and CT scans. Here we report on our development of a THz tomography system, with potential uses in the nondestructive imaging of Army platforms.

The fundamental idea in 2-D tomography (creating a tomographic image in the $xy$ plane of Fig. 1) is that we can acquire spectra for points along the $x$ axis and through different $\theta$ angles from 0° to 180°. For 3-D tomography, collecting spectra along the third axis (the $z$ axis) allows us to combine multiple 2-D images to create a 3-D image. Experimentally, it is important to keep track of the rotation center: the simplest way to do so is to collect data along the $x$ axis such that the origin is in the center of the $x$ axis raster.

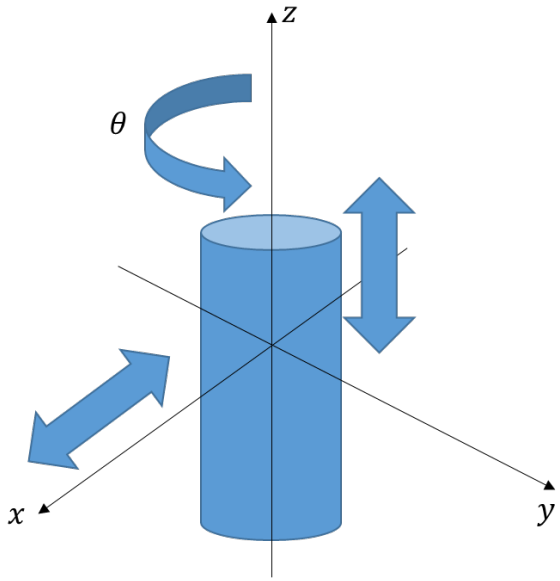


**Fig. 1 Scanning directions for a THz tomography system. The sample is rastered along three linear directions $x, y, z$ and one angular direction $\theta$. A THz spectrum is taken at each point.**

Mathematically, the sample is defined by a function $\alpha(x, y)$, which is the distribution of the material's absorption coefficient over the shape of the sample. Let us also define a line $L(l, \theta)$ by two parameters $l$ and $\theta$ (Fig. 2). The parameter $l$ describes the offset from the origin, and the parameter $\theta$ describes the angle of incidence. If an incident beam of intensity $I_0$ travels through the line $L(l, \theta)$, the transmitted beam, assuming a Beer's Law attenuation model, is

$$I_L = I_0 e^{-\int_{L(l,\theta)} \alpha \, dL} \quad . \tag{1}$$

In Eq. 1, $\int_{L(l,\theta)} \alpha \, dL$ is the line integral of the absorption coefficient over the line $L(l, \theta)$.

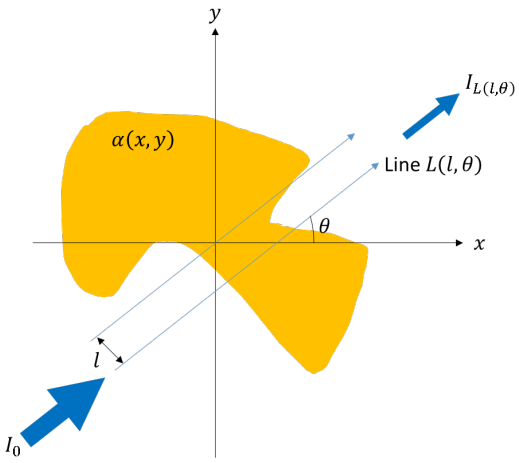


**Fig. 2 Mathematical principle behind tomography**

Reparametrizing the line integral gives

$$\int_{L(l,\theta)} \alpha \, dL = \iint_{-\infty}^{\infty} \alpha(x, y) \delta(x \cos(\theta) - y \sin(\theta) - l) \, dx dy. \tag{2}$$

Experimentally, the THz emitter provides $I_0$ and we can measure $I_{L(l,\theta)}$ for several angles $\theta$ and offsets $l$. If we plot the measured $-\ln\left(\frac{I_{L(l,\theta)}}{I_0}\right)$ ratio for each line $L(l, \theta)$, we obtain a sinogram $S(l, \theta)$:

$$S(l, \theta) = \ln\left(\frac{I_0}{I_{L(l,\theta)}}\right) = \iint_{-\infty}^{\infty} \alpha(x, y) \delta(x \cos(\theta) - y \sin(\theta) - l) \, dx dy. \tag{3}$$

Experimentally, we must keep track of $(l, \theta)$ for each THz spectrum, thus necessitating that we keep track of the center of rotation. Equation 3 is a functional transform, called the Radon transform $\mathcal{R}$:

$$S(l, \theta) = \mathcal{R}\{\alpha(x, y)\}. \tag{4}$$

$S(l,\theta)$ is experimentally determined. So, the mathematical problem is to find $\alpha(x,y)$ when given $S(l,\theta)$. This is accomplished with the inverse Radon transform:

$$\alpha(x,y) = \mathcal{R}^{-1}\big(S(l,\theta)\big). \tag{5}$$

We implement the inverse Radon transform via the filtered back projection algorithm. Essentially, with the filtered back projection algorithm, we can relate the sinogram to the 2-D Fourier transform of $\alpha$. We can then inverse Fourier transform to obtain $\alpha$ in real space. Other inverse Radon transform algorithms exist, each with their own advantages and disadvantages.[6,7]

## 2. Experimental

To demonstrate the utility of THz TDS as a tomographic investigation tool, we imaged the internal structure of a pencil sharpener. We scanned from 0° to 180° in 10° increments, giving us different $\theta$ values. Scanning beyond 180° is unnecessary because 10° and 190° incident rays travel the same path through the sample (Fig. 2). The sample was rastered in the $x$ direction (giving us different $l$ values, Fig. 2) and in the $z$ direction increments (giving several different 2-D cross sections). Without a motorized angular stage, the entire process is quite time consuming.

From each THz TDS spectra, we can determine the ratio $\frac{I_0}{I_{L(l,\theta)}}$. $I_0$ is taken to be the maximum peak-to-peak amplitude in free space and $I_{L(l,\theta)}$ is taken to be the maximum peak-to-peak amplitude at the scan through the line $L(l,\theta)$ (Fig. 3). The sinogram $S(l,\theta)$ for the pencil sharpener and the inverse Radon transformed reconstruction are shown in Fig. 4.

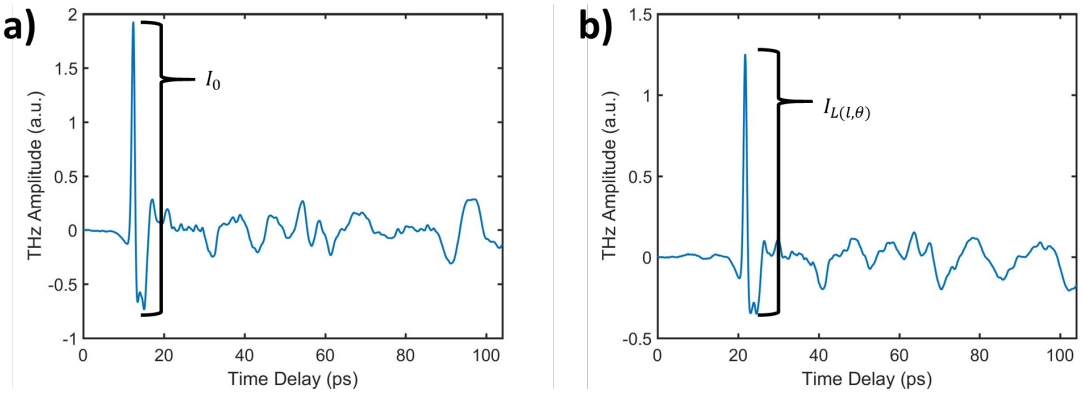


**Fig. 3 a) THz time domain pulse through free space and b) THz time domain pulse traveling through the line $L(l,\theta)$. The delay in the $L(l,\theta)$ pulse and the decay in the amplitude are due to traveling through material.**

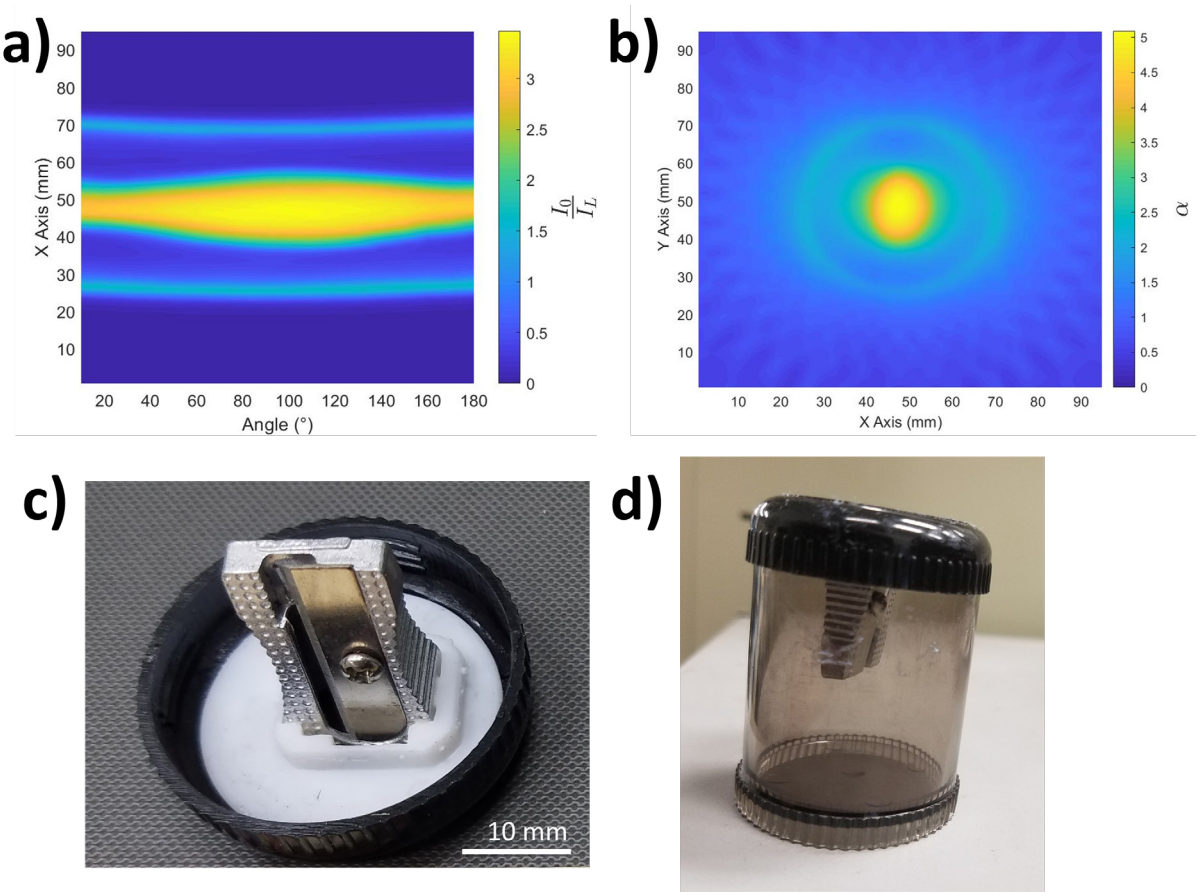


**Fig. 4 a) Sinogram of the pencil sharpener, b) inverse Radon transformed sinogram to reconstruct qualitative absorption coefficient, and c) and d) pencil sharpener used in these experiments**

In Fig. 4b, the scale bar is qualitatively related to absorption index. For example, the high absorption middle is due to the oblong metallic piece in the pencil sharpener: while the metal does not necessarily absorb THz radiation, it does not transmit THz. The dark blue regions do not absorb any THz radiation—they are air. The circular outline in Fig. 4b is due to increased absorption from the plastic container. The lines present in Fig. 4b are due to insufficient angular sampling.

By rastering the THz system in the *z* direction, we can achieve 2-D scans at varying heights to create a 3-D rendering. The rendering in Fig. 5 was produced by plotting an isosurface of the data in Fig. 4b. In Fig. 5, the red portion corresponds to the metallic centerpiece and the blue portion corresponds to the plastic surrounding the sharpener.

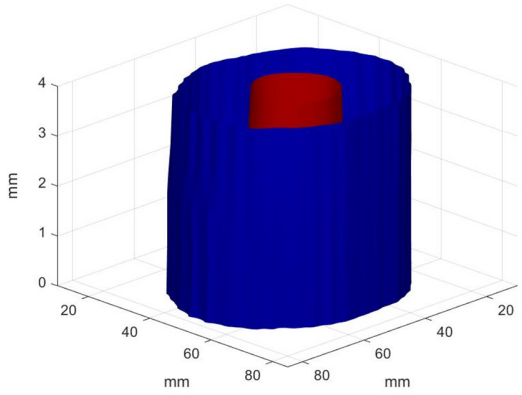


**Fig. 5 3-D rendering of the THz tomography pencil sharpener. The red portion corresponds to the metallic center piece and the blue portion corresponds to the plastic surrounding the sharpener.**

## 3. THz Tomography for Nondestructive Evaluation of 3-D-Printed Devices

One of the potential applications of THz tomography is for the nondestructive evaluation of 3-D-printed devices. It is often difficult, but very important, to inspect the internal structure of such devices. Here, we aim to use THz tomography to investigate the internal structure of a 3-D-printed polymer cube. The results are shown in Fig. 6.

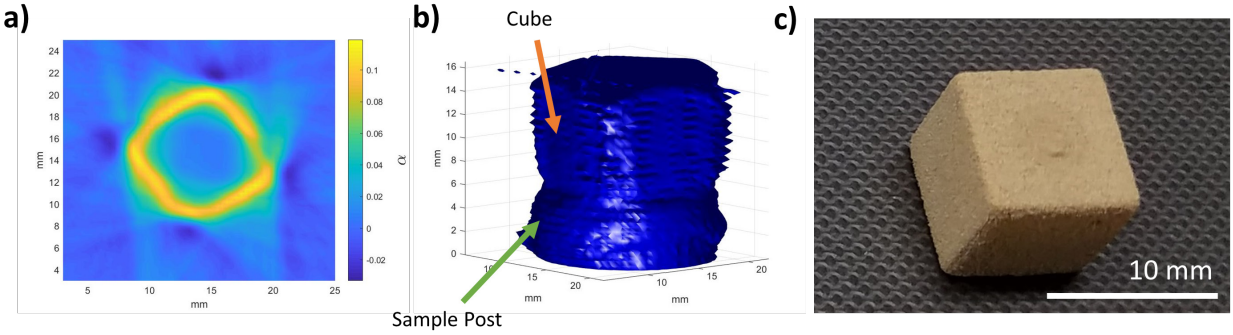


**Fig. 6 a) Cross-sectional view of the 3-D-printed cube, b) 3-D isosurface rendering, and c) polymer cube**

Figure 6a shows a cross-sectional view of the polymer cube. While a rough outline of the square cube can be seen, the internal structure is computed to be hollow, which is certainly not the case. The cause seems to be that cube edges lead to greater THz scattering. Figure 6b shows the isosurface 3-D rendering, and Fig. 6c shows the polymer cube used.

We also compared the THz tomography with X-ray microtomography, which is shown in Fig. 7. The resolution of the X-ray microtomography allows for the

detection of micrometer-scale pores, which we cannot detect with THz TDS. The diffraction-limited resolution of THz tomography and insufficient sampling limits our ability to adequately detect small defects in this approach.

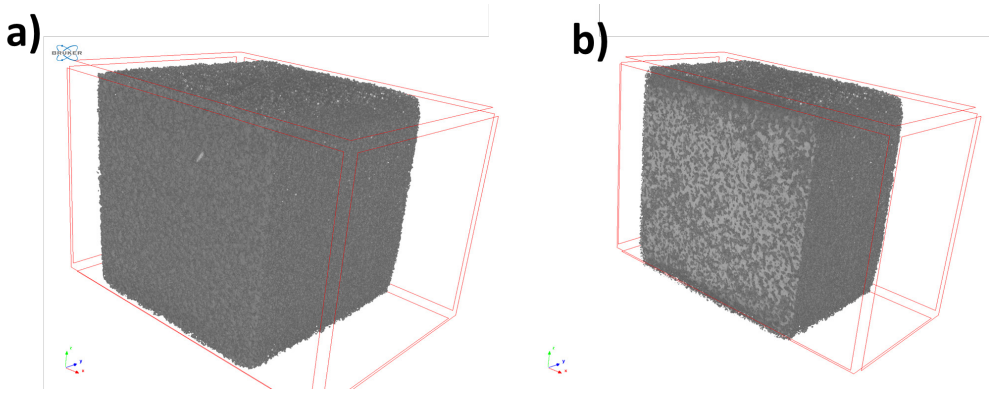


**Fig. 7 X-ray microtomography of the polymer cube in Fig. 6c**

## 4. Conclusions

Here, we have implemented a THz tomography system. We have demonstrated the ability of the system to reproduce cross-sectional images of objects. Yet, the utility of the system is thus far limited by the diffraction limit of the THz waves and the size of the objects being imaged. A small (~10 mm) 3-D-printed polymer cube was imaged using both THz and X-ray tomography. The THz tomography system was unable to successfully reproduce the cross-sectional view of the polymer cube but was able to reproduce the outline of the polymer cube. Overall, THz tomography has many potential applications, but resolution limitations in current configuration have to be taken into account. These limitations could be potentially overcome by implementation of resolution enhancement techniques such as metamaterial lens or moving to higher operation at higher THz frequencies.

## 5. References


1. Semenov S. Microwave tomography: review of the progress towards clinical applications. Philosophical Transactions of the Royal Society A: Mathematical, Physical and Engineering Sciences. 2009;367(1900):3021–3042. doi: 10.1098/rsta.2009.0092.

2. Zhu YK, Tian GY, Lu RS, Zhang H. A review of optical NDT technologies. Sensors (Basel). 2011;11(8):7773–7798.

3. Brahm A, Knuz M, Riehemann S, Notni G, Tünnermann A. Volumetric spectral analysis of materials using terahertz-tomography techniques. Applied Physics B. 2010;100(1):151–158.

4. Recur B, Desbarats P, Domenger J-P, Guillet J-P, Bassel L, Fragnol C, Manek-Hönninger IB, Delagnes J-C, Benharbone W, Mounaix P. Terahertz radiation for tomographic inspection. SPIE Optical Engineering. 2012;51:9:091609-1–091609-7.

5. Wang S, Zhang XC. Pulsed terahertz tomography. Journal of Physics D: Applied Physics. 2004;37(4):R1.

6. Guillet JP, Recur B, Frederique L, Bousquet B, Canioni L, Manek-Hönninger IB, Desbarats P, Mounaix P. Review of terahertz tomography techniques. Journal of Infrared, Millimeter, and Terahertz Waves. 2014;35(4):382–411.

7. Recur B, Younus A, Salort S, Mounaix P, Chassagne B, Desbarats P, Caumes J-P, Abraham E. Investigation on reconstruction methods applied to 3D terahertz computed tomography. Optics Express. 2011;19(6):5105–5117.

## List of Symbols, Abbreviations, and Acronyms

| | |
|---|---|
| 2-D, 3-D | two-dimensional, three-dimensional |
| CT | computed tomography |
| MRI | magnetic resonance imaging |
| TDS | time domain spectroscopy |
| THz | terahertz |

| | |
|---|---|
| 1 (PDF) | DEFENSE TECHNICAL INFORMATION CTR DTIC OCA |
| 1 (PDF) | CCDC ARL FCDD RLD CL TECH LIB |
| 1 (PDF) | GOVT PRINTG OFC A MALHOTRA |
| 1 (PDF) | CCDC ARL FCDD RLW ME D SHREIBER |